

The scaling properties of dissipation in incompressible isotropic three-dimensional magnetohydrodynamic turbulence

J. A. Merrifield

Department of Physics, University of Warwick, Coventry CV4 7AL, United Kingdom

W.-C. Müller

Max-Planck-Institut für Plasmaphysik, 85748 Garching, Germany

S. C. Chapman^{a)}

Department of Physics, University of Warwick, Coventry CV4 7AL, United Kingdom

R. O. Dendy^{b)}

UKAEA Culham Division, Culham Science Centre, Abingdon, Oxfordshire OX14 3DB, United Kingdom

(Received 28 September 2004; accepted 8 November 2004; published online 5 January 2005)

The statistical properties of the dissipation process constrain the analysis of large scale numerical simulations of three-dimensional incompressible magnetohydrodynamic (MHD) turbulence, such as those of Biskamp and Müller [Phys. Plasmas **7**, 4889 (2000)]. The structure functions of the turbulent flow are expected to display statistical self-similarity, but the relatively low Reynolds numbers attainable by direct numerical simulation, combined with the finite size of the system, make this difficult to measure directly. However, it is known that extended self-similarity, which constrains the ratio of scaling exponents of structure functions of different orders, is well satisfied. This implies the extension of physical scaling arguments beyond the inertial range into the dissipation range. The present work focuses on the scaling properties of the dissipation process itself. This provides an important consistency check in that we find that the ratio of dissipation structure function exponents is that predicted by the She and Leveque [Phys. Rev. Lett **72**, 336 (1994)] theory proposed by Biskamp and Müller. This supplies further evidence that the cascade mechanism in three-dimensional MHD turbulence is nonlinear random eddy scrambling, with the level of intermittency determined by dissipation through the formation of current sheets.

© 2005 American Institute of Physics. [DOI: 10.1063/1.1842133]

I. INTRODUCTION

This paper investigates the previously underexplored topic of scaling in the local rate of dissipation in magnetohydrodynamic (MHD) flows. Turbulent fluids and plasmas display three properties that motivate development of statistical theories:¹ (i) disorganization, in the sense that structures arise on all scales; (ii) unpredictability of detailed behavior, in the sense of inability to predict a signal's future behavior from knowledge of its past, implying links with deterministic chaos; and (iii) reproducibility of statistical measures, combined with the presence of statistical self-similarity. Much progress has been made by the heuristic treatment of scaling laws derived from energy cascade arguments, following Kolmogorov and Richardson, see, for example, Ref. 1. The basic idea is that energy-carrying structures (eddies) are injected on large scales, nonlinear eddy interaction causes energy to cascade to smaller scales in a self-similar manner, and energy is finally dissipated by viscosity on small scales. A quasistationary state evolves where the rate of viscous dissipation matches the rate of energy injection. Scaling exponents ζ_p characterize the resulting statistical self-similarity found in structure functions S_l^p :

$$S_l^p = \langle (\mathbf{v}(\mathbf{x} + \mathbf{l}, t) \cdot \mathbf{l} / l - \mathbf{v}(\mathbf{x}, t) \cdot \mathbf{l} / l)^p \rangle \sim l^{\zeta_p}. \quad (1)$$

Here \mathbf{v} is the fluid velocity, \mathbf{x} is a position vector, \mathbf{l} is a differencing vector, and the average is an ensemble average. The statistical self-similarity represented by the power law in l is only valid within the inertial range $l_d \ll l \ll l_0$; here l_0 is the characteristic macroscale, and l_d is the dissipation scale at which the cascade terminates. The set of scaling exponents ζ_p in Eq. (1) is expected to be universal since it characterizes the generic cascade process. It is worth noting here that universality can only be expected in the isotropic case. When anisotropies are present, deviation from the isotropic case can be expected, and this will relate to the strength of the anisotropy. In MHD turbulence, anisotropy can be introduced in the form of an imposed magnetic field. The effect of this on the scaling exponents is investigated in Ref. 2. This reference also investigates anisotropy in terms of that introduced by the local magnetic field even when an applied field is absent. This stems from the Goldreich and Sridhar objection to the assumption of local isotropy in the MHD case.³ In Ref. 2 structure functions are calculated with the differencing length perpendicular and parallel to the local magnetic field. The perpendicular structure functions were found to exhibit stronger intermittency than the parallel structure functions. Exponents calculated from the perpendicular structure functions were found to coincide with those calculated from the

^{a)}Also at Radcliffe Institute, Harvard University, Cambridge, MA, USA.

^{b)}Also at Department of Physics, University of Warwick, Coventry CV4 7AL, UK.

isotropic structure functions. Essentially dimensional arguments, in which the relevant physical parameters are identified heuristically, have been formulated to provide basic fluid scaling information. These arguments linearly relate ζ_p to p , for example, the Kolmogorov 1941 phenomenology^{4,5} predicts $\zeta_p = p/3$. As such, basic fluid scaling can be characterized by one number a such that

$$S_l^p \sim l^{pa}. \quad (2)$$

To exploit these concepts, let us write the equations of incompressible MHD in Elsässer symmetric form:⁶

$$\begin{aligned} \partial_t \mathbf{z}^\pm = & -\mathbf{z}^\mp \cdot \nabla \mathbf{z}^\pm - \nabla(p + B^2/2) + (\nu/2 + \eta/2)\nabla^2 \mathbf{z}^\pm \\ & + (\nu/2 - \eta/2)\nabla^2 \mathbf{z}^\mp, \end{aligned} \quad (3)$$

$$\nabla \cdot \mathbf{z}^\pm = 0. \quad (4)$$

Here the Elsässer field variables are $\mathbf{z}^\pm = \mathbf{v} \pm \mathbf{B}(\mu_0 \rho)^{-1/2}$, where p is the scalar pressure, ν is kinematic viscosity, η is magnetic diffusivity, and ρ is fluid density. The symmetry of Eq. (3) suggests that statistical treatment of \mathbf{z}^\pm may be more fundamental than separate treatments of \mathbf{v} and \mathbf{B} . In light of this, longitudinal structure functions are constructed in terms of Elsässer field variables hereafter:

$$S_l^{p(\pm)} = \langle (\mathbf{z}^\pm(\mathbf{x} + \mathbf{l}, t) \cdot \mathbf{l} / l - \mathbf{z}^\pm(\mathbf{x}, t) \cdot \mathbf{l} / l)^p \rangle \sim l^{\zeta_p^{(\pm)}}. \quad (5)$$

As mentioned above, heuristic arguments that make predictions about basic fluid scaling only linearly relate ζ_p to p . In reality ζ_p depends nonlinearly on p due to the intermittent spatial distribution of eddy activity. Basic fluid scaling can be modified to take this into account by the application of an intermittency correction. A commonly applied class of intermittency correction describes statistical self-similarity in the local rate of dissipation ϵ_l by means of scaling exponents τ_p :

$$\begin{aligned} \langle \epsilon_l^p \rangle \equiv & \left\langle \left(\frac{\nu}{4\pi l^3} \int_0^l \frac{1}{2} (\partial_i v_j(x + l', t) + \partial_j v_i(x \right. \right. \\ & \left. \left. + l', t))^2 dl'^3 \right)^p \right\rangle \sim l^{\tau_p}. \end{aligned} \quad (6)$$

For a review of the fractal nature of the local rate of dissipation for hydrodynamics, see, for example, Ref. 7

As we shall see, the intermittent nature of the system is captured by the nonlinear dependence of ζ_p on p in Eq. (6). This nonlinearity can conveniently be expressed multiplicatively in relation to the basic linear fluid scaling of Eq. (2). Specifically we may write

$$S_l^p \sim \langle \epsilon_l^{gp} \rangle l^{ap}, \quad (7)$$

where g is a constant whose value is inferred from model assumptions such as those of Kolmogorov and Iroshnikov–Kraichnan.^{8,9} This is Kolmogorov's refined similarity hypothesis.⁵ The scaling exponents ζ_p in Eq. (5) are inferred by Eq. (7) to be $\zeta_p = \zeta_{pg} + pa$. That is, the intermittency in the velocity field structure functions is achieved via reasoning concerning local rate of dissipation. One model that uses this hypothesis, and has proven successful in predicting the scaling exponents for hydrodynamic turbulence, is that from the 1994 paper of She and Leveque (SL).¹⁰ Here

physical assumptions are made regarding the scaling of the local rate of dissipation. Specifically: the hierarchical nature of Eq. (6) above, as expressed in Eq. (6) of Ref. 10; the rate of dissipation by the most intensely dissipating structures is related only to the eddy turnover time as determined by the basic fluid scaling, as in Eq. (5) of Ref. 10; and the space filling nature of the most intensely dissipating structures can be described by one parameter (their Hausdorff dimension). These three assumptions can be combined to formulate a second-order difference equation for the scaling exponents τ_p that has one nontrivial solution, as in Eq. (9) of Ref. 10. This solution can be formulated in terms of the two parameters: the codimension of the most intensely dissipating structures, $C = D - d_H$, where D is the embedding dimension and d_H is the Hausdorff dimension; and the basic fluid scaling number expressed by a in Eq. (2) above. Following Ref. 10, we may write

$$\tau_p = -(1-a)p + C - C(1 - (1-a)/C)^p. \quad (8)$$

This two parameter formulation follows that previously noted by Dubrulle,¹¹ whose parameters Δ and β correspond to our $(1-a)$ and $1 - \Delta/C$, respectively. The refined similarity hypothesis, as expressed in Eq. (7), is then invoked to obtain the following expression for the structure function scaling exponents ζ_p :

$$\zeta_p = pa - (1-a)pg + C - C(1 - (1-a)/C)pg. \quad (9)$$

Previously Elsässer field structure functions have been identified with a SL model of the type Eq. (9), see, for example, Refs. 12–14. In the present paper the refined similarity hypothesis for MHD is tested by applying a modified form of Eq. (7), see Eq. (12), to the simulation data of Biskamp and Müller. This provides an important consistency check for previous studies. Equation (8), which probes the multifractal properties of the local rate of dissipation, but does not rely on the refined similarity hypothesis, can also be tested directly against the simulation results, as we discuss below.

Direct numerical simulations must resolve the dissipation scale l_d so that energy does not accumulate at large wave numbers, artificially stunting the cascade. Most of the numerical resolution is therefore used on the dissipation range, whereas it is only on scales much larger than l_d that dissipative effects are negligible, and scaling laws of the type discussed arise. Thus high Reynolds number simulations with an extensive inertial range are currently unavailable. However, the principle of extended self-similarity (ESS) (Ref. 15) can be used to extend the inertial range scaling laws into the range of length scales that is significantly affected by dissipation but still larger than l_d . Instead of considering the scaling of individual structure functions, the principle of ESS involves investigating the scaling of one order structure function against another, on the assumption that

$$S_l^{p(\pm)} \sim (S_l^{q(\pm)})^{(\zeta_p/\zeta_q)}. \quad (10)$$

Here it can be seen that any set of structure functions will satisfy this relation providing

$$S_l^p \sim G(l)^{\zeta_p}, \quad (11)$$

where $G(l)$ can be any function of l which is independent of p . Here we use the notation of Emily *et al.* that these authors used to describe the general properties of generalized extended self-similarity, as expressed in Eq. (8) of Ref. 16—though generalized ESS is not discussed in the present paper. When the objective of ESS is to extend scaling into the dissipation range, $G(l)$ can be rewritten as $l^{G'(l)}$, where $G'(l)$ is introduced to accommodate the nonconstant flux of energy through length scales in the dissipation range. As such, $G'(l)$ asymptotically approaches one as the length scale increases from the dissipative to the inertial range.

The She–Leveque model as it has appeared so far is only valid in the inertial range. Let us now discuss how this model can be interpreted in the framework of ESS. For example, this problem has been tackled for hydrodynamic turbulence by Dubrulle.¹¹ In that paper the explicit inclusion of l in the refined similarity hypothesis [Eq. (7) with $g = \Delta = 1/3$ for hydrodynamic turbulence] is replaced by a generalized length scale, which is cast in terms of the third order structure function as expressed in Eq. (12) of Ref. 11. This problem was addressed similarly by Benzi *et al.* where the scaling relation

$$S_l^p \sim \langle \epsilon_l^{gp} \rangle (S_l^{1/a})^{pa} \quad (12)$$

is explicitly formulated in Ref. 17. The appropriate relation between ζ_p and τ_p is now $\zeta_p = \tau_{pg} + pa\zeta_{1/a}$. Using this relation combined with Eq. (11) and (12) it can be seen that $\langle \epsilon_l^p \rangle$ must also have the form $\langle \epsilon_l^p \rangle \sim G(l)^{\tau_p}$. This implies ESS exists also in the local rate of dissipation, such that

$$\langle \epsilon_l^p \rangle \sim \langle \epsilon_l^q \rangle^{(\tau_p/\tau_q)}. \quad (13)$$

It can then be seen that if a She–Leveque model of the general type Eq. (9) is used to explain scaling exponents obtained via ESS, as expressed in Eq. (10), then two consistency checks are appropriate. First Kolmogorov's refined similarity hypothesis should be satisfied in the form Eq. (12), and second ESS should exist in the local rate of dissipation as in Eq. (13).

The present paper performs these checks for consistency for the simulation of Biskamp and Müller.¹³ Here the scaling exponents $\zeta^{(\pm)}$ [see Eq. (5)] were investigated via direct numerical simulation of the three-dimensional (3D) incompressible MHD equations, with a spatial grid of 512³ points.^{13,18} The simulation is of decaying turbulence with initially equal magnetic and kinetic energy densities and $\nu = \eta$. A fuller discussion of the numerical procedure is present in the following section. Since the turbulence decays with time, structure functions are normalized by the total energy in the simulation (kinetic plus magnetic) before time averaging takes place. Biskamp and Müller¹³ extracted the ratios of scaling exponents ζ_p/ζ_3 by ESS and directly determined $\zeta_p \approx 1$. These exponents were found to match a variant of the She–Leveque 1994 model Eq. (9) inserting Kolmogorov basic fluid scaling ($g = a = 1/3$) with the most intensely dissipating structures being sheetlike ($C = 1$). Early investigations of this type assumed Iroshnikov–Kraichnan fluid scaling where the most intensely dissipating structures are sheetlike (see Refs. 12 and 19), making $g = a = 1/4$ and $C = 1$. Sheetlike in-

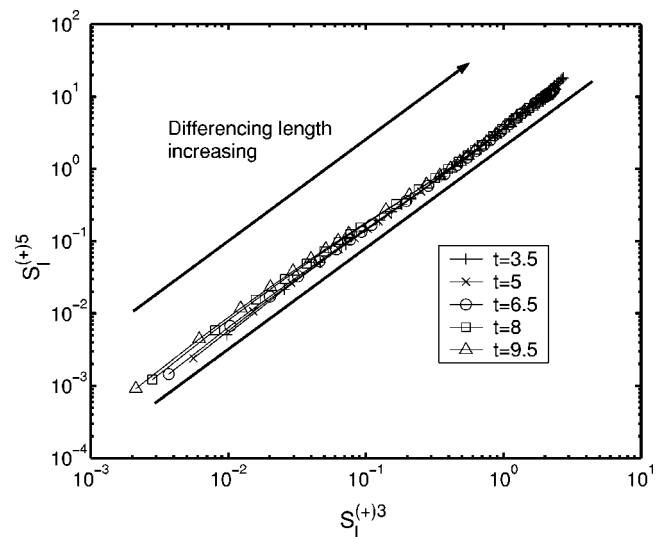


FIG. 1. Extended self-similarity for the Elsässer field variable $\mathbf{z}^{(+)}$ (order 5 against order 3), compare Eq. (10), for decaying MHD turbulence where structure functions are normalized by the total energy before time averaging. This normalization reveals the same underlying scaling for points from different simulation times, as shown, after Biskamp and Müller (Ref. 13).

tensely dissipating structures are thought to exist in MHD turbulence because of the propensity of current sheets to form. We refer to Fig. 5 of Ref. 13 for isosurfaces of current density squared, and to Fig. 2 for isosurfaces constructed from the shear in the $\mathbf{z}^{(+)}$ field $(\partial_i z_i^{(+)})^2$. Both figures show the existence of two dimensional coherent structures; Fig. 2 is more directly related to the analyses presented in the present paper. Basic Kolmogorov fluid scaling for Alfvénic fluctuations has been verified for low Mach number (≈ 0.1) compressible^{14,20} and incompressible^{13,18} 3D MHD turbulence by power spectrum analysis, and by checking for scaling in the third order structure function such that $\zeta_3 = 1$. Extended self-similarity has also been utilized to extract ratios of scaling exponents related to an inverse cascade in laboratory plasmas.²¹ In other work, a generalized version of this SL model has been applied to compressible flows where C is allowed to vary as a fitting parameter,^{14,22} and in the case of Ref. 22 this dimension is interpreted as a function of the sonic Mach number. Figure 1 shows an example of the normalization and ESS procedure for $\mathbf{z}^{(+)}$ structure functions from the data analyzed here.

The philosophy behind our investigation can now be summarized as follows. Given a simulation, the set of structure functions S_l^p can be calculated. These are expected to display statistical self-similarity as expressed in Eq. (5), where the scaling exponents ζ_p give insight into the physics of the cascade process. The relatively low Reynolds numbers attainable by direct numerical simulation, combined with the finite size of the system, make this statistical self-similarity difficult to measure directly. However, it is found that extended self-similarity of the type expressed in Eq. (10) is well satisfied, allowing the ratio of scaling exponents ζ_p/ζ_3 to be directly measured. There is a range of *a priori* views concerning these ratios, reflecting physical model assumptions. The ratios of scaling exponents recovered from ESS

analysis of the 3D MHD simulation data are compared with these models, and the best fit is identified. Our investigation thus assists in validating the physical assumptions made in formulating the currently favored model, namely, Eq. (9) with $g=a=1/3$ and $C=1$ giving $\zeta_p=p/9+1-(1/3)^{p/3}$. In particular, we confirm the existence of a specific type of extended self-similarity in the local rate of dissipation, with exponents given by Eq. (8) with $a=1/3$ and $C=1$ giving $\tau_p=-2p/3+1-(1/3)^p$. We also show that Kolmogorov's refined similarity hypothesis, in the form Eq. (12), is satisfied.

II. NUMERICAL PROCEDURES

The data analyzed here stems from a direct numerical simulation of decaying isotropic turbulence (see Ref. 13 for additional details). The equations of incompressible MHD are written in terms of the vorticity, $\omega=\nabla\times\mathbf{v}$, in order to eliminate the pressure variable. These are solved by a pseudospectral scheme (see, for example, Ref. 23). Time integration is carried out by applying the trapezoidal leapfrog method.²⁴ The aliasing error associated with this approach²⁵ is reduced to discretization error level by spherical truncation of the Fourier grid.²⁶

The simulation domain comprises a periodic box in Fourier space with 512^3 points. Initially the fields have random phases and amplitudes $\sim\exp[-k^2/(2k_0^2)]$ with $k_0=4$. The ratio of total kinetic and magnetic energy of the fluctuations is set to one. Cross helicity, which is proportional to $\int_V[(\mathbf{z}^+)^2-(\mathbf{z}^-)^2]dV$, is absent throughout the duration of the simulation. The magnetic helicity, $H^M=1/2\int_V\mathbf{A}\cdot\mathbf{B}dV$, where $\mathbf{B}=\nabla\times\mathbf{A}$, is set to $0.7H_{\max}^M$. Here $H_{\max}^M\simeq E^M/k_0$ where E^M is the energy in the magnetic field. The diffusivities $\nu=\eta=4\times 10^{-4}$ imply a magnetic Prandtl number $Pr_m=\nu/\eta$ of one.

The run was performed over ten eddy turnover times, defined as the time required to reach maximum dissipation when starting from smooth initial fields. Structure functions and moments of dissipation are calculated in time intervals of 0.5 between $t=3.5$ and $t=9.5$, during which the turbulence undergoes self-similar decay.

III. RESULTS

In the present paper, the gradient squared measure $(\partial_i z_i^{(\pm)})^2$ is used as a proxy⁵ for the local rate of dissipation $(\partial_i B_j - \partial_j B_i)^2 \eta/2 + (\partial_i v_j + \partial_j v_i)^2 \nu/2$. This proxy has recently been employed to study turbulence in the thermal ion velocity of the solar wind as measured by the Advanced Composition Explorer (ACE) spacecraft,²⁷ giving results consistent with those presented below. This is particularly interesting insofar as the solar wind remains one of the few accessible system of quasistationary fully developed MHD turbulence⁶ although we note that MHD intermittency studies have also been performed on the reversed field pinch experiment.²⁸ Figure 2 shows isosurface plots of the gradient squared measure for the simulation of Biskamp and Müller. Two dimensional coherent structures dominate the image, suggesting the dimension parameter entering an SL model should equal two, as in the model employed by Biskamp and Müller. Following Eq. (6), statistical self-similarity in the dissipation measure is expressed as

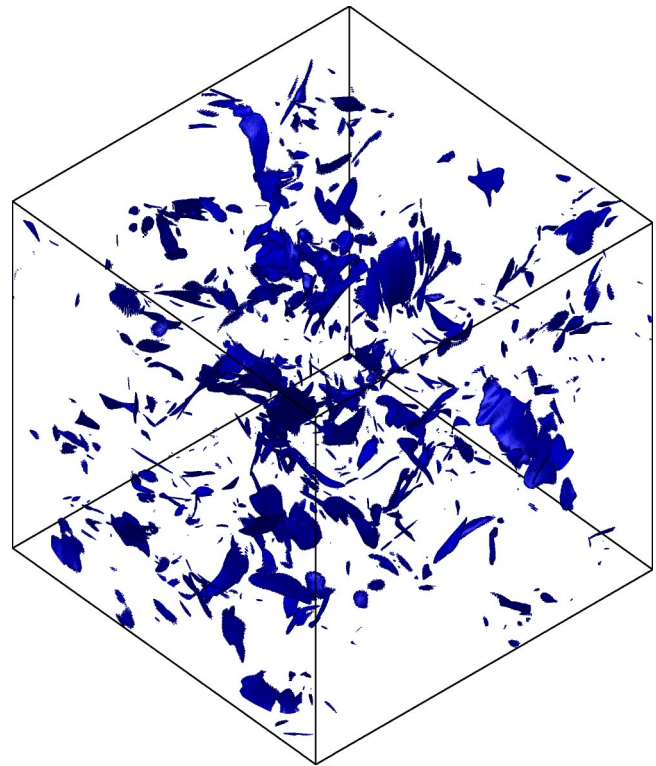


FIG. 2. (Color online) Isosurfaces of sheetlike (2D) coherent structures of the squared gradient of the $\mathbf{z}^{(+)}$ Elsässer field variable from the 3D MHD turbulence simulation of Biskamp and Müller.

$$\chi_l^{p(\pm)} \equiv \left\langle \left(\frac{1}{l} \int_0^l [\partial_i z_i^{(\pm)}(x+l',t)]^2 dl' \right)^p \right\rangle \sim l^{\tau_p^{(\pm)}}. \quad (14)$$

This proxy, which involves a one-dimensional integration rather than the full 3D integration of Eq. (6), facilitates comparison with related experimental MHD (Refs. 21 and 27) and hydrodynamic^{7,17,29} studies, and also offers benefits in computation time.

The SL model adopted by Biskamp and Müller predicts

$$\tau_p^{(\pm)} = -2p/3 + 1 - (1/3)^p. \quad (15)$$

This is simply Eq. (8) with $a=1/3$ and $C=1$. Gradients are calculated from the data of Biskamp and Müller¹³ using a high order finite difference scheme, and the integral is performed by the trapezium method. Normalization by the spatial average of viscous plus Ohmic rates of dissipation allows time averaging to be performed. Figure 3 shows an example of the ESS and normalization procedure for $\chi_l^{p(+)}$ order $p=5$ against order $p=3$. Statistical self-similarity is recovered with roll-off from power-law scaling as l approaches the system size. This roll-off behavior at large l may be due to the finite size of the system, since a more extensive part of the simulation domain is encompassed by the spatial average (the integral over dl') as l increases in Eq. (14). In Fig. 3 points identified with this roll-off are removed, and ratio of scaling exponents (τ_p/τ_3) is calculated from the remaining points by linear regression. These ratios are shown in Fig. 4. No significant difference between the scaling recovered from $\mathbf{z}^{(+)}$ and $\mathbf{z}^{(-)}$ can be seen. This should be expected since no theoretical distinction needs to be drawn between $\mathbf{z}^{(+)}$ and

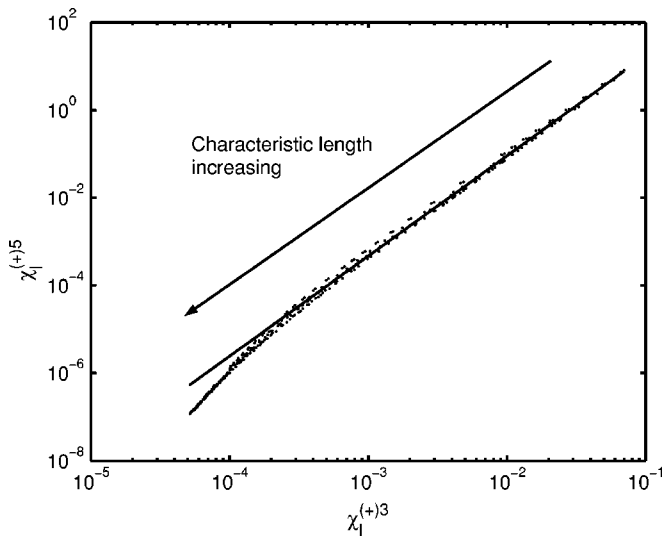


FIG. 3. Extended self-similarity in the Elsässer field variable $\mathbf{z}^{(+)}$ gradient squared proxy for the local rate of dissipation (order 5 against order 3), compare Eq. (13) with the gradient squared proxy from Eq. (14) replacing ϵ_l^v . Normalization by the space averaged local rate of viscous and Ohmic dissipation allows time averaging in spite of the decay process. Deviation from power-law scaling at large l is probably a finite size effect. The solid line is the best fit in the linear region.

$\mathbf{z}^{(-)}$ for the vanishing values of cross helicity present in this simulation. The solid line in Fig. 4 shows the ratio predicted by Eq. (15), in contrast to the dashed line which shows the ratio predicted by the SL theory for hydrodynamic turbulence.¹⁰ Caution must be taken when calculating high order moments, since these are strongly influenced by the tails of their associated distributions. This can easily lead to bad counting statistics. The order p is only taken up to $p = 6.5$ for the dissipation measure (instead of $p=8$ as for the Elsässer field structure functions¹³ because of the extremely

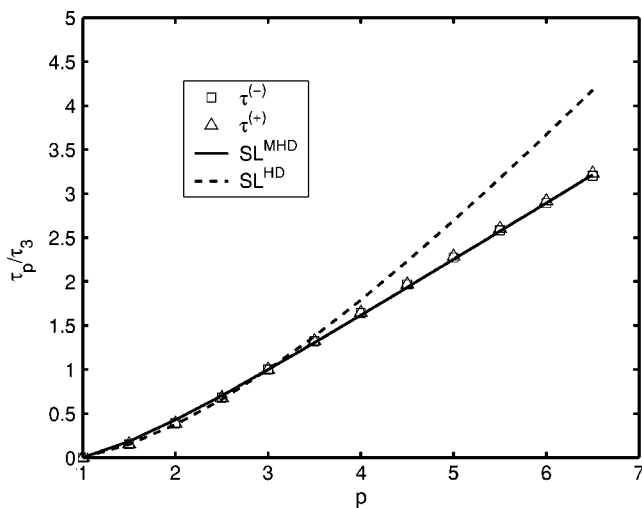


FIG. 4. Ratio of scaling exponents (order p over order 3) obtained via extended self-similarity from the Elsässer field gradient squared proxy for the local rate of dissipation. Errors in these measurements lie within the marker symbols. Solid line shows ratios predicted by a She–Leveque theory based on Kolmogorov fluid scaling and sheetlike most intensely dissipating structures, Eq. (15). The dashed line shows ratios predicted by hydrodynamic She–Leveque (Ref. 10).

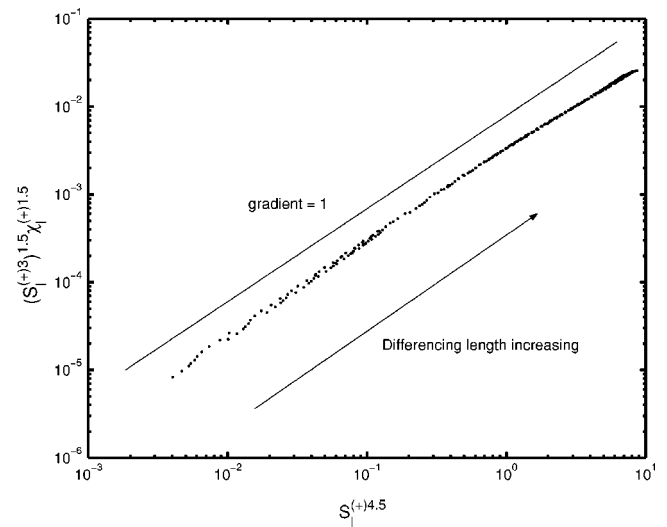


FIG. 5. Plot to test Kolmogorov’s refined similarity hypothesis as applied to extended self-similarity, Eq. (12). This involves taking the product of the field variable and dissipative structure functions, in contrast to Figs. 1 and 3. Agreement with the hypothesis would give a straight line with unit gradient. Normalization was performed as in Figs. 1 and 3 to allow time averaging despite the decay process.

intermittent nature of the signal; large values affect the average [the angular brackets in Eq. (14)] more as the order p increases. This effect is evaluated using a similar methodology to that in Ref. 30. If a worst case scenario is imagined, where the average is strongly affected by one point in the signal, one would expect $l/\delta l$ members of the spatial average in Eq. (14) to be directly affected by this point, where δl is the grid spacing. We can then define an event as incorporating $l/\delta l$ members of the spatial average. It is found that $\approx 5\%$ of the average is defined by only approximately ten events for order $p=6.5$. This situation is of course worse for higher values of p .

Plots were constructed in order to test Eq. (12). This involves taking the product of structure functions of the field

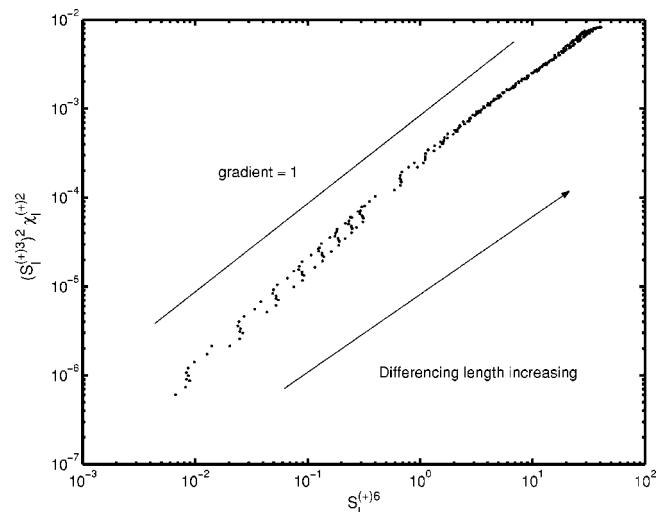


FIG. 6. High order test of Kolmogorov’s refined similarity hypothesis as applied to extended self-similarity, Eq. (12). Normalization is performed as in Fig. 5.

variables and the dissipative quantities, in contrast to Figs. 1 and 3. Figures 5 and 6 show these plots for $n=1.5$ and $n=2$, respectively. The low order measure in Fig. 5 shows a relation that is nearly linear, with a gradient close to the ideal value of one, see Eq. (12). This is encouraging considering the deviation expected at the smallest and largest scales due to finite size effects. However, unlike the case in Fig. 3, there may be some curvature across the range of the plot. The higher order measure in Fig. 6 deviates from a linear scaling relation. We note that taking this test to high order involves the product of two quantities that have challenging counting statistics, plotted against a high order structure function. The deviation of the gradient seen in Fig. 6 from the ideal value of one is perhaps not surprising, because the constraints described above become stronger at high order.

IV. CONCLUSIONS

Extended self-similarity is recovered in the gradient squared proxy for the local rate of dissipation of the Elsässer field variables $\mathbf{z}^{(\pm)}$ computed by Biskamp and Müller. We believe this is the first time this has been shown for MHD flows. This result supports the application to Elsässer field scaling exponents $\zeta_p^{(\pm)}$ of turbulence theories that require statistical self-similarity in the local rate of dissipation, even when $\zeta_p^{(\pm)}$ are extracted from relatively low Reynolds number flows via ESS. Furthermore the ratio of exponents recovered is that predicted by the SL theory proposed by Biskamp and Müller.¹³ This supplies further evidence that the cascade mechanism in three-dimensional MHD turbulence is nonlinear random eddy scrambling, with the level of intermittency determined by dissipation through the formation of two dimensional coherent structures. However, Kolmogorov's ESS modified refined similarity hypothesis remains to be verified at high order.

ACKNOWLEDGMENTS

The authors are grateful to Tony Arber for helpful discussions.

This research was supported in part by the United Kingdom Engineering and Physical Sciences Research Council. S.C.C. acknowledges a Radcliffe fellowship.

- ¹U. Frisch, *Turbulence* (Cambridge University Press, Cambridge, UK, 1995).
- ²W.-C. Müller, D. Biskamp, and R. Grappin, Phys. Rev. E **67**, 066302 (2003).
- ³P. Goldreich and S. Sridhar, Astrophys. J. **438**, 763 (1995).
- ⁴A. N. Kolmogorov, Proc. R. Soc. London, Ser. A, London Ser. A **434**, 9 (1991).
- ⁵K. R. Sreenivasan and R. A. Antonia, Annu. Rev. Fluid Mech. **29**, 435 (1997).
- ⁶D. Biskamp, *Nonlinear Magnetohydrodynamics* (Cambridge University Press, Cambridge, UK, 1993).
- ⁷C. Meneveau and K. R. Sreenivasan, J. Fluid Mech. **224**, 429 (1991).
- ⁸P. S. Iroshnikov, Sov. Astron. **7**, 566 (1964).
- ⁹R. H. Kraichnan, Phys. Fluids **8**, 1385 (1964).
- ¹⁰Z.-S. She and E. Leveque, Phys. Rev. Lett. **72**, 336 (1994).
- ¹¹B. Dubrulle, Phys. Rev. Lett. **73**, 959 (1994).
- ¹²H. Politano and A. Pouquet, Phys. Rev. E **52**, 636 (1995).
- ¹³D. Biskamp and W.-C. Müller, Phys. Plasmas **7**, 4889 (2000).
- ¹⁴N. Haugen, A. Brandenburg, and W. Dobler, Phys. Rev. E **70**, 678 (2002).
- ¹⁵R. Benzi, S. Ciliberto, R. Tripiccion, C. Baudet, F. Massaioli, and S. Succi, Phys. Rev. E **48**, R29 (1993).
- ¹⁶S. C. Emily, Z.-S. She, S. Weidong, and Z. Zhengping, Phys. Rev. E **65**, 066303 (2002).
- ¹⁷R. Benzi, S. Ciliberto, C. Baudet, and G. R. Chavarría, Physica D **80**, 385 (1995).
- ¹⁸W.-C. Müller and D. Biskamp, Phys. Rev. Lett. **84**, 475 (2000).
- ¹⁹R. Grauer, J. Krug, and C. Marliani, Phys. Lett. A **195**, 335 (1994).
- ²⁰A. N. S. Boldyrev and P. Padoan, Astrophys. J. **573**, 678 (2002).
- ²¹G. Y. Antar, Phys. Rev. Lett. **91**, 055002 (2003).
- ²²P. Padoan, R. Jimenez, A. Nordlund, and S. Boldyrev, Phys. Rev. Lett. **92**, 191102 (2004).
- ²³C. Canuto, M. Y. Hussaini, A. Quarteroni, and T. A. Zang, *Spectral Methods in Fluid Dynamics* (Springer, New York, 1988).
- ²⁴Y. Kurihara, Mon. Weather Rev. **93**, 33 (1965).
- ²⁵S. A. Orszag, Stud. Appl. Math. **51**, 253 (1972).
- ²⁶A. Vincent and M. Meneguzzi, J. Fluid Mech. **225**, 1 (1991).
- ²⁷A. Bershadskii, Phys. Plasmas **10**, 4613 (2003).
- ²⁸V. Carbone, L. Sorriso-Valvo, E. Martinez, V. Antoni, and P. Veltri, Phys. Rev. E **62**, R49 (2000).
- ²⁹G. R. Chavarría, C. Baudet, and S. Ciliberto, Phys. Rev. Lett. **74**, 1986 (1995).
- ³⁰T. S. Horbury and A. Balogh, Nonlinear Processes Geophys. **4**, 185 (1997).